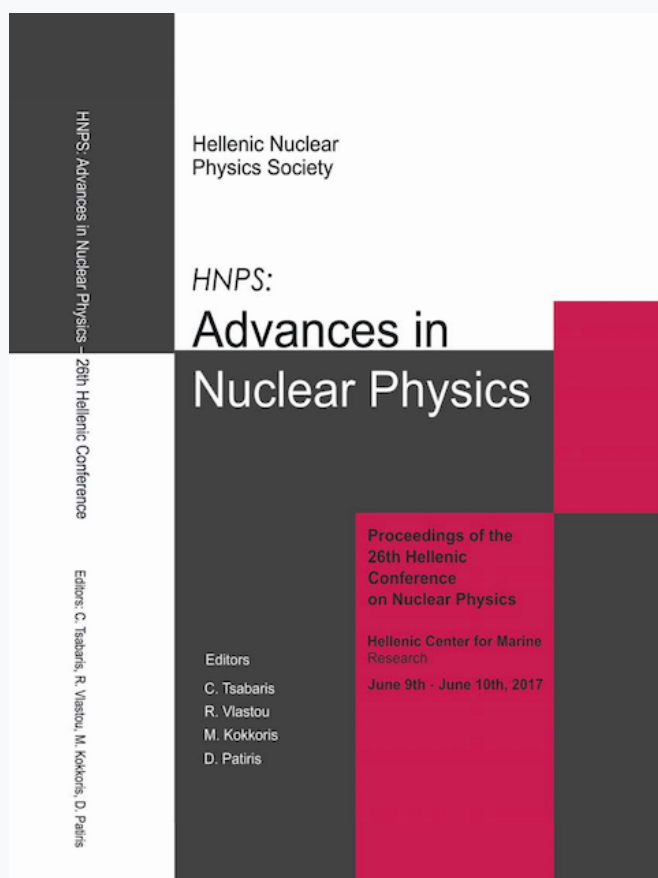


HNPS Advances in Nuclear Physics

Vol 25 (2017)

HNPS2017



Measurement of the differential cross sections of ${}^6,{}^7\text{Li}(d,d0){}^6,{}^7\text{Li}$ for Ion Beam Analysis purposes

E. Ntemou, X. Aslanoglou, M. Axiotis, V. Foteinou, M. Kokkoris, A. Lagoyannis, P. Misaelides, N. Patronis, K. Preketes-Sigalas, G. Provatas, R. Vlastou

doi: [10.12681/hnps.1974](https://doi.org/10.12681/hnps.1974)

To cite this article:

Ntemou, E., Aslanoglou, X., Axiotis, M., Foteinou, V., Kokkoris, M., Lagoyannis, A., Misaelides, P., Patronis, N., Preketes-Sigalas, K., Provatas, G., & Vlastou, R. (2019). Measurement of the differential cross sections of ${}^6,{}^7\text{Li}(d,d0){}^6,{}^7\text{Li}$ for Ion Beam Analysis purposes. *HNPS Advances in Nuclear Physics*, 25, 208–214. <https://doi.org/10.12681/hnps.1974>

Measurement of the differential cross sections of ${}^{6,7}\text{Li}(\text{d},\text{d}_0){}^{6,7}\text{Li}$ for Ion Beam Analysis purposes

E. Ntemou^{1,2,*}, X. Aslanoglou³, M. Axiotis², V. Foteinou², M. Kokkoris¹, A. Lagoyannis², P. Misaelides⁴, N. Patronis³, K. Preketes–Sigalas^{1,2}, G. Provas², R. Vlastou¹

¹*Department of Physics, National Technical University of Athens, Zografou Campus 157 80, Athens, Greece*

²*Institute of Nuclear and Particle Physics, NCSR ‘Demokritos’, Aghia Paraskevi 153 10, Greece*

³*Department of Physics, University of Ioannina, Ioannina, Greece*

⁴*Department of Chemistry, Aristotle University of Thessaloniki, Thessaloniki, Greece*

Abstract In the present work, the ${}^{6,7}\text{Li}(\text{d},\text{d}_0){}^{6,7}\text{Li}$ elastic scattering differential cross sections were determined in the deuteron energy range $E_{\text{lab}}=900\text{--}2000$ keV for elastic backscattering spectroscopy (EBS) purposes, using thin lithium targets, made by evaporating natural (${}^{\text{nat}}\text{LiF}$) and isotopically enriched (${}^6\text{LiF}$) powder on self-supporting carbon foils and with an ultra-thin Au layer on top for normalization purposes. The experiment was carried out in deuteron beam energy steps of 5 or 30 keV and for the laboratory scattering angles of 125° , 140° , 150° , 160° , and 170° .

Keywords EBS; ${}^6\text{Li}$; ${}^7\text{Li}$; Differential cross sections

INTRODUCTION

The accurate quantitative determination and concentration depth profiling of lithium is important for the characterization of a great variety of materials, ranging from glass and ceramics to metallic alloys and polymers. Natural lithium is composed of two isotopes, $\sim 92.5\%$ ${}^7\text{Li}$ and $\sim 7.5\%$ ${}^6\text{Li}$, whose relative mass difference is high and taking into consideration the different applications of each isotope, ${}^7\text{Li}$ is used at liquid fluoride nuclear reactors, whereas ${}^6\text{Li}$ has a very high neutron cross-section (~ 940 barns) and so readily fissions to yield tritium and helium, one reaches to the conclusion that their individual analytical study is imperative.

However, the depth profiling of Li presents a strong analytical challenge for all IBA (Ion Beam Analysis) techniques, since it is highly reactive and, due to its low atomic number, is usually present in relatively complex matrices along with several medium-Z or high-Z elements. In the field of NRA (Nuclear Reaction Analysis), the most promising reactions seem to be the ${}^6\text{Li}(\text{d},\text{a}_0)[1]$, the ${}^6\text{Li}(\text{d},\text{p}_0)[2]$ and the ${}^6\text{Li}(\text{p},{}^3\text{He})[3]$ ones. The latter two are particularly important, not only because they yield isolated peaks with practically no background (due to the high Q-values involved), but mainly due to the fact that d-NRA can facilitate the simultaneous study of practically all the main light isotopes possibly coexisting

* Corresponding author, email: ntemou@inp.demokritos.gr

in a target.

The applicability of d–NRA would be greatly enhanced if one could also simultaneously analyze the resulting EBS (Elastic Backscattering Spectroscopy) spectra using the same experimental setup and conditions in a coherent way. However, as evidenced in IBANDL (Ion Beam Analysis Nuclear Data Library, <https://www-nds.iaea.org/exfor/ibandl.htm>), there is a complete lack of relevant deuteron elastic scattering differential cross-section datasets on $^{6,7}\text{Li}$, for low energies particularly suitable for IBA, namely below $E_{d,\text{lab}} \sim 2.2$ MeV, where the inevitable neutron background remains low.

Thus, the present work aims at contributing in this field, by providing the $^{6,7}\text{Li}(d,d_0)^{6,7}\text{Li}$ elastic scattering differential cross sections, measured in the energy range $E_{\text{lab}} = 900 - 2000$ keV, using thin lithium targets, made by evaporating $^{\text{nat}}\text{LiF}$ and isotopically enriched ^6LiF powders on self-supporting carbon stripping foils, with an ultra-thin Au layer on top for charge normalization purposes. The experiment was carried out in deuteron beam energy steps of 5 to 30 keV, depending on the fine structure of each studied cross section, and for the laboratory scattering angles of 125° , 140° , 150° , 160° , and 170° .

EXPERIMENTAL DETAILS

The experiment was conducted at the 5.5 MV Tandem accelerator of the Institute of Nuclear and Particle Physics (INPP), National Center of Scientific Research (NCSR) “Demokritos”, using deuterons in the energy range $E_{d,\text{lab}} = 900\text{--}2000$ keV in steps of 5–30 keV. The accelerator beam energy was determined by means of the narrow resonance of the $^{27}\text{Al}(p, \gamma)^{28}\text{Si}$ reaction at $E_p = 991.9$ keV [4] and the energy ripple was calculated to be $\sim 0.1\%$. The deuterons passed through a 2 mm collimator and end up in a cylindrical chamber of large dimensions ($R \sim 40$ cm) where the targets were placed in the center of the goniometer and the target holder was mounted perpendicular to the beam axis. The targets were constructed at the Tandem laboratory using the evaporation technique. Firstly, a small quantity of natural ($^{\text{nat}}\text{LiF}$) and isotopically enriched (^6LiF) powder (97% in ^6Li) was evaporated on self-supporting carbon foils and an ultra-thin Au layer was subsequently evaporated on top for normalization purposes. For the estimation of the target thickness and the enrichment of the ^6LiF target complementary measurements were carried out using the proton beam at the energies $E_p = 1600, 1700$ keV.

The detection system was composed of five Si surface barrier detectors (SSB) with 500 μm thickness and ~ 13 keV resolution (value acquired from a polished Si target), which were placed at the laboratory scattering angles of 125° , 140° , 150° , 160° , and 170° with respect to the beam direction, at a distance of ~ 10 cm from the target. In front of each detector vertical slits (~ 2 mm in width) were placed in order to minimize the angular uncertainty ($\sim 1^\circ$) and small aluminum tubes (length of 3–8 cm in length, 1 cm in diameter) were placed in front of the detectors in order to minimize the number of detected counts due to multiply-scattered ions from the chamber walls. The beam current on the target did not exceed 70 nA to avoid

excessive pile-up effects and to prevent damage on the thin target due to overheating. The data acquisition was accomplished using standard NIM electronics.

The SPECTRW code [5] was used for the peak integration and background subtraction and the new version of SIMNRA, v.6.94, capable of treating narrow resonances [6], was used for the analysis of certain EBS spectra (effects of multiple and plural scattering, ZBL stopping power data and Chu and Yang's straggling model were used as implemented in the code).

DATA ANALYSIS, RESULTS AND DISCUSSION

The determination of the cross-section values for both isotopes of lithium (${}^6\text{Li}$, ${}^7\text{Li}$) was accomplished using the relative measurement technique, thus the following formula was used:

$$\left(\frac{d\sigma}{d\Omega}\right)_{\theta,E}^{6,7\text{Li}} = \left(\frac{d\sigma}{d\Omega}\right)_{\theta,E'}^{\text{Au}} \times \frac{Y_{6,7\text{Li}}}{Y_{\text{Au}}} \times \frac{N_{\text{Au}}}{N_{6,7\text{Li}}}$$

where, E corresponds to the energy at the half of the target's thickness, E' corresponds to the corrected beam energy at the surface of the target, $\left(\frac{d\sigma}{d\Omega}\right)_{\theta,E_2}^{\text{Au}}$ corresponds to the differential cross section of Au, which was calculated using the Rutherford scattering formula along with screening effects for the specific beam energy range, Y to the integrated area of each peak (using spectrW) and N to the layer thickness, in at/cm².

Lithium 6 case

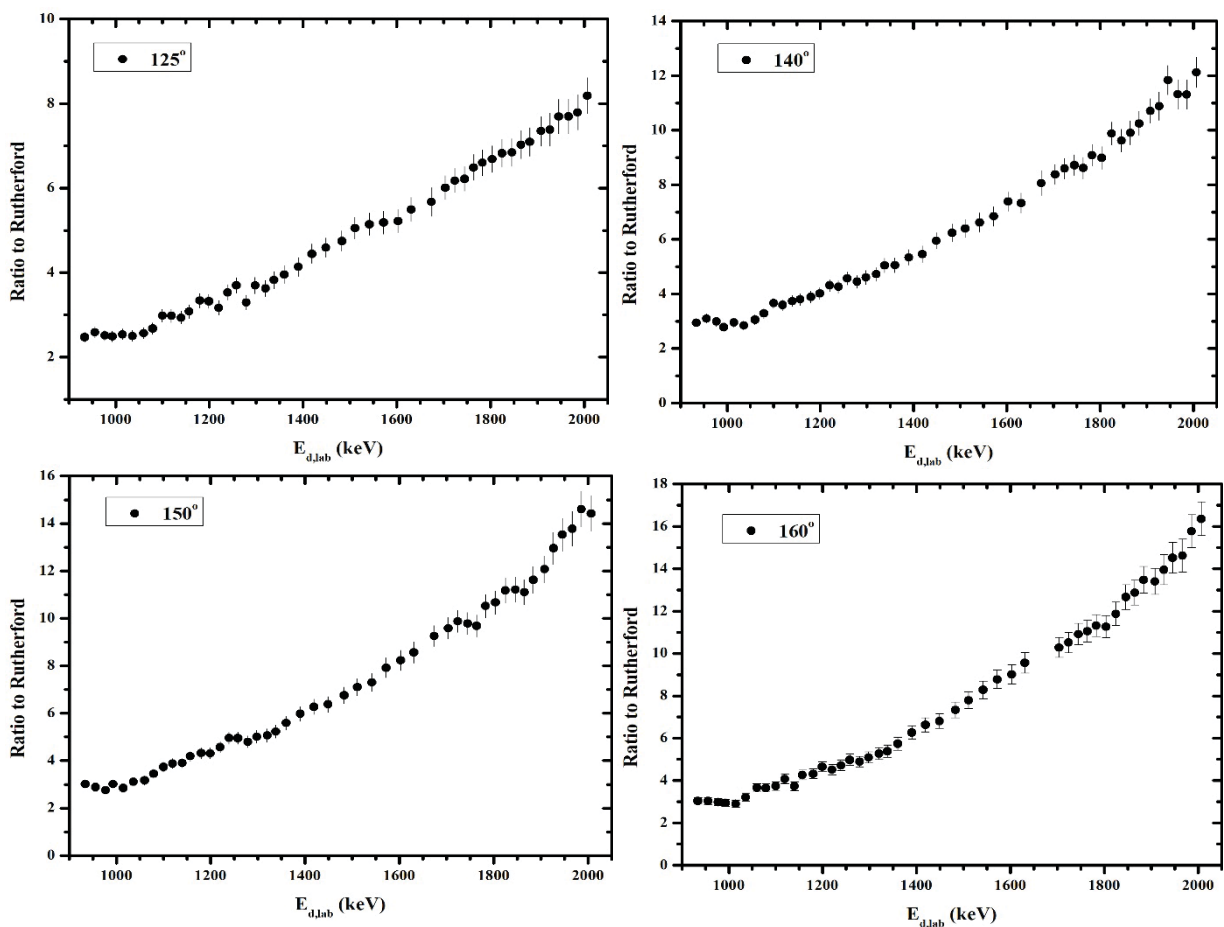
For the lithium 6 case, in order to calculate the ${}^6\text{Li}$:Au areal surface density ratio the following assumption was made: Lithium and fluorine maintain their respective elemental ratio (namely $\frac{N_{\text{Au}}}{N_{\text{Li}}} = \frac{N_{\text{Au}}}{N_{\text{F}}}$) due to the strong chemical bond of LiF during evaporation.

Moreover, the equation $\frac{N_{\text{Au}}}{N_{\text{Li}}} = \frac{N_{\text{Au}}}{N_{\text{Li}} * f_{\text{enrich}}}$ holds (where f_{enrich} is the enrichment factor of ${}^6\text{Li}$ in the target), and by using the assumption made above the following equation can be derived:

$\frac{N_{\text{Au}}}{N_{6\text{Li}}} = \frac{N_{\text{Au}}}{N_{\text{Li}} * f_{\text{enrich}}} = \frac{N_{\text{Au}}}{N_{19\text{F}} * f_{\text{enrich}}}$. For the target thickness calculation the last equation was utilized

along with deuteron spectra up to ~1200 keV because, as shown in [7], the deuteron elastic scattering from fluorine follows the Rutherford formula especially for the case of the scattering angles of 140° and 150°, (deviations are less than 2%). Thus, the target thickness was obtained by fitting the low-energy deuteron spectra at 1160 and 1200 keV using the SIMNRA program (v. 6.94). The results of this procedure yield a mean value of $\frac{N_{\text{Au}}}{N_{\text{Li}}} = 0.091 \pm 0.004$, namely a statistical uncertainty of the order of 5% (this value excludes all possible systematic uncertainties due to the adopted approach). Moreover, during the target thickness calculation process different stopping power compilations were utilized and the discrepancies were always below 1%.

Furthermore, the enrichment factor needed to be determined. For this purpose, the proton EBS spectra were used at $E_{p,lab}=1600$ keV and 1700 keV in five scattering angles (125° , 140° , 150° , 160° , 170°). More specifically, proton spectra of both the enriched target ${}^6\text{LiF}$ and the natLiF target were used and the ratios $\frac{Y_{nat}^{6\text{Li}}}{Y_{en}^{6\text{Li}}}$ and $\frac{Y_{nat}^F}{Y_{en}^F}$ were determined. Subsequently, thickness and charge normalization processes were carried out and, taking into account that the abundance of ${}^6\text{Li}$ in ${}^{nat}\text{Li}$ is 7.5%, the average value of the enrichment factor was obtained as 97%, with a statistical error of $\sim 2\%$. This experimental value was adopted for the determination of the differential cross-section values, as it was in excellent agreement with the nominal one supplied by the manufacturer.



Figs. 1a-d. Differential cross-section values to the ones derived from the Rutherford formula of the ${}^6\text{Li}(d,d_0){}^6\text{Li}$ elastic scattering, measured at deuteron energies $E_{lab}=940\text{--}2000$ keV and for the scattering angles of 125° , 140° , 150° , 160° in variable energy steps. The total estimated uncertainties are included in the graphs; in the x-axis the error bars are not visible due to the selected scale.

Typical examples of the obtained differential cross-section values to the ones derived from the Rutherford formula for the elastic scattering process ${}^6\text{Li}(d,d_0){}^6\text{Li}$ and for four backscattering angles (125° , 140° , 150° , 160°) are presented in Figs.a–d. The total uncertainty budget did not exceed 5.5% in all cases. The error bars concerning the beam energy are not

visible in the x-axis in the figures, due to the selected scale. It should be noted however, that a 2.7% mean deviation exists between the SRIM compilation and the existing experimental stopping power data for lithium, while for fluorine, according to the SRIM website (<https://www.srim.org>), there is no information available. The energy values correspond to the half of the target thickness and were calculated using the SIMNRA code implementing ZBL stopping power data.

As shown in Figs. 1a-d, large deviations from the Rutherford formula (in some cases up to a factor of ~ 15) can be observed. Specifically, in the low-energy region (930–980 keV) there seems to be a tail of a resonance for the detector angles of 125° , 140° , 150° , 160° which can be attributed to the level of the compound nucleus ^8Be with energy $E_x^* = 22240$ keV and amplitude $\Gamma = 800$ keV. This level is below the energy range studied in the present work but it affects the cross-section values due to its large amplitude. Concerning the whole structure of the cross-section values, it may be explained by the broad overlapping levels of ^8Be with energies $E_x^* = 22240$ keV, 22980 keV, and 24000 keV and amplitudes $\Gamma = 800$ keV, 230 keV and 7000 keV respectively, which are all out of the energy range studied in the present work.

Lithium 7 case

For the case of lithium 7, the target thickness was determined using the same final equation that was used for the lithium 6 case. However, in this particular case, the enrichment factor was well known, as is the abundance of lithium 7 to natural lithium, namely 0.9241 and the equation used is $\frac{N_{\text{Au}}}{N_{^7\text{Li}}} = \frac{N_{\text{Au}}}{N_{\text{Li}} \cdot 0.9241} = \frac{N_{\text{Au}}}{N_{^{19}\text{F}} \cdot 0.9241}$. The obtained mean value is 0.0084 ± 0.0004 , which introduces a statistical uncertainty $\sim 4.8\%$ in the final cross-section values (excluding systematics namely stopping power data).

It should be mentioned here that during the integration process a complication occurred; at several energies ($E_{d,\text{lab}} < \sim 1300$ keV) and angles there was a full or partial overlap between the $^{12}\text{C}(d,p_1)$, $^7\text{Li}(d,d_0)$ and $^7\text{Li}(d,p_0)$ peaks, as shown in Fig. 2.

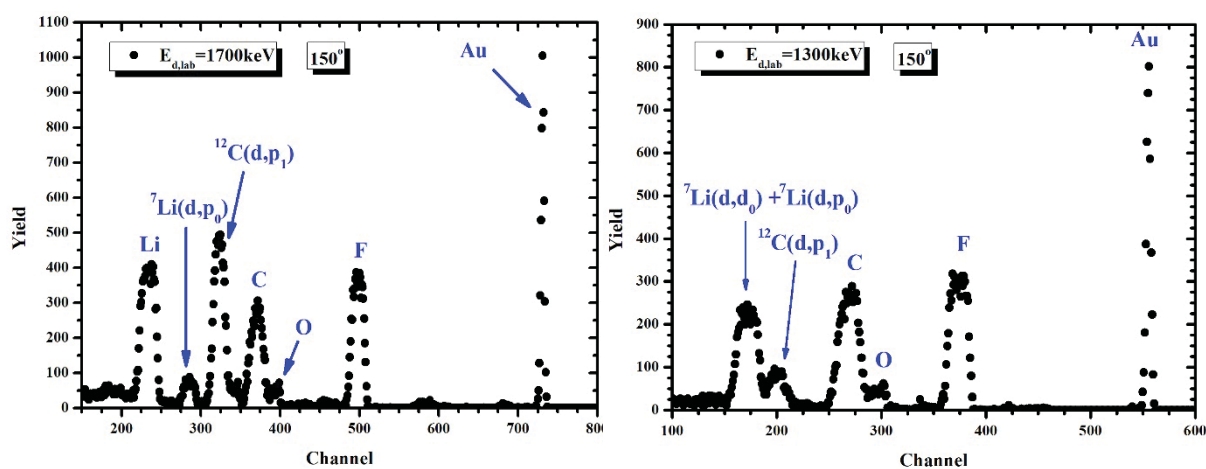
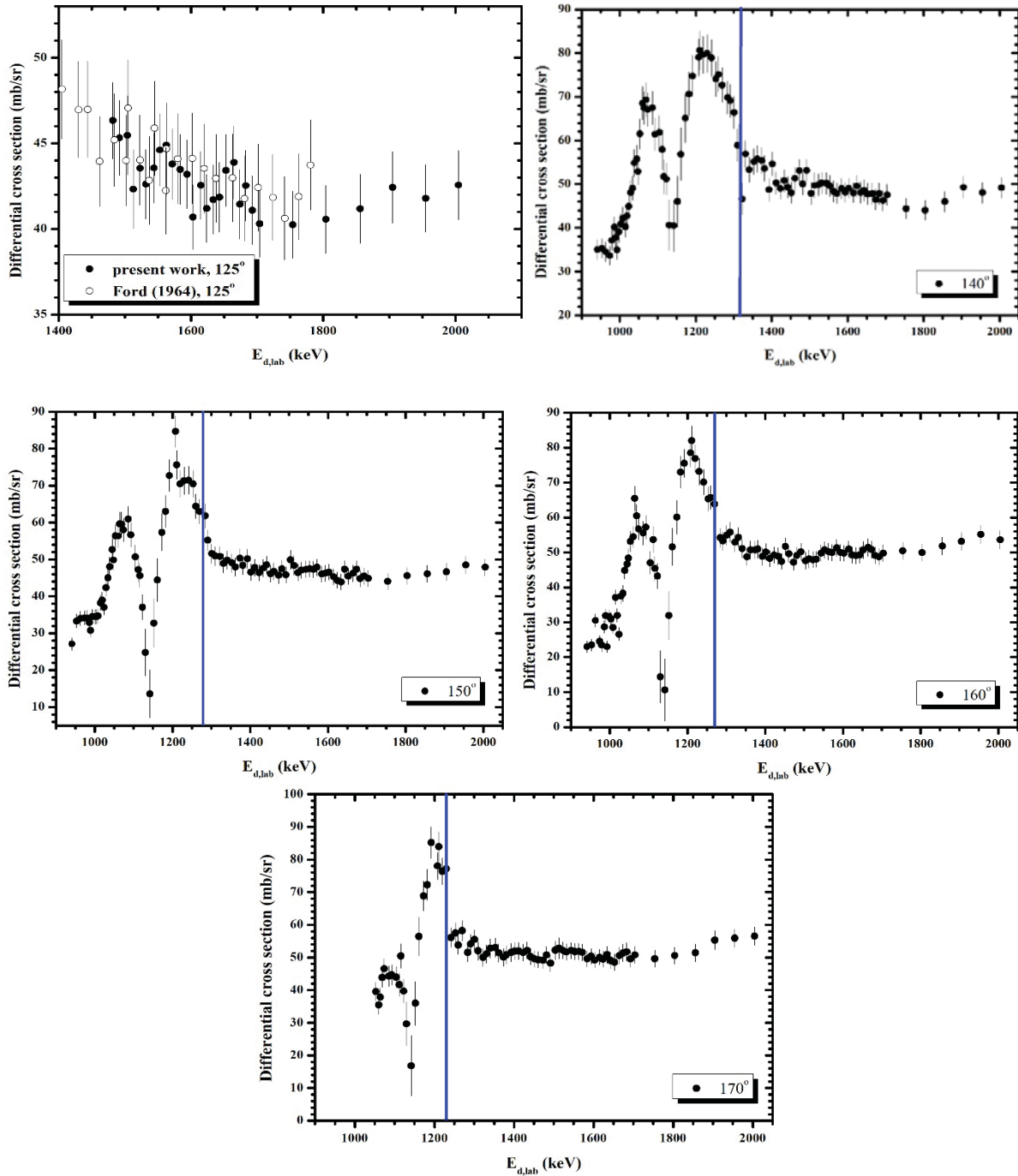


Fig. 2 Typical experimental spectra for the energy $E_{d,\text{lab}} = 1700$ keV at 140° and $E_{d,\text{lab}} = 1300$ keV at 150° along with the corresponding peak identification. At the latter spectrum the overlap of the peaks is visible.

Thus, in order to overcome this problem, firstly the amount of carbon in the target was calculated using the evaluated SigmaCalc [8] data for the $^{12}\text{C}(d,d_0)$ and $^{12}\text{C}(p,p_0)$ reactions and the experimental peaks and subsequently the $^{12}\text{C}(d,p_1)$ data from Kokkoris et al. [9] were utilized for the extraction of the $^{12}\text{C}(d,p_1)$ counts from the total counts in the sum peak (except for the case of 125° where no experimental data exists) using SIMNRA.



Figs. 3a-d. Differential cross-section values of the $^7\text{Li}(d,d_0)^7\text{Li}$ elastic scattering from the blue line and for higher energies and differential cross-section values for the sum of $^7\text{Li}(d,d_0)^7\text{Li}$ and $^7\text{Li}(d,p_0)^7\text{Li}$, measured at deuteron energies $E_{lab}=940\text{--}2000$ keV and for the scattering angles of 125° , 140° , 150° , 160° , 170° , in variable energy steps. The total estimated uncertainties are included in the graphs; in the x-axis the error bars are not visible due to the selected scale.

Furthermore, for the case of 140° , data from Kokkoris et al. taken at 145° were used due to the relative invariance of the angular distribution (within $\pm 10^\circ$) of the $^{12}\text{C}(d,p_1)$ reaction at low deuteron beam energies. Experimental data for the $^7\text{Li}(d,p_0)$ reaction does not exist in the literature and therefore this procedure was impossible for this reaction. However, in case of in-situ measurements this overlap would also appear and thus the obtained results can be useful. The differential cross-section values for the $^7\text{Li}(d,d_0)$ elastic scattering are presented in Fig.3a-d along with the total uncertainties, where from the blue line and for lower energies the experimental values correspond to the sum of the $^7\text{Li}(d,d_0)$ and $^7\text{Li}(d,p_0)$ whereas from the blue line and for higher energies the experimental values correspond only to the $^7\text{Li}(d,d_0)$ elastic scattering.

The total uncertainties of the experimental cross-section values are $\sim 6\text{-}15\%$ for the low beam energies and $\sim 5\%$ for the high beam energies. This difference in the two areas is caused by the subtraction of the counts from the $^{12}\text{C}(d,p_1)$ reaction and the uncertainty originates from the uncertainty of the cross-section values for the $^{12}\text{C}(d,p_1)$ reaction. The structure of the cross-section values that is visible in the low energy region may be attributed to the superposition of the resulting yield of $^7\text{Li}(d,d_0)$ and $^7\text{Li}(d,p_0)$ reactions due to the level with energy $E_{\text{cm}}=17495$ keV ($\Gamma=47$ keV) of the compound nucleus, ^9Be . Moreover, the high values of the determined differential cross sections, which are more than 5 and up to ~ 23 times greater than the ones obtained using Rutherford's formula, indicate that the $^7\text{Li}(d,d_0)$ is suitable for the concentration determination of lithium.

CONCLUSIONS

In the present work the differential cross sections of the deuteron elastic scattering on both isotopes of lithium ($^6,^7\text{Li}(d,d_0)$) were determined for the beam energy range $E_{d,\text{lab}}=900\text{-}2000$ keV, in steps between 5 and 50 keV, and for the five detection angles 125° , 140° , 150° , 160° and 170° , which are widely used for EBS measurements. In the case of ^7Li and for low beam energies, the combined differential cross sections for both $^7\text{Li}(d,d_0)$ and $^7\text{Li}(d,p_0)$ reactions have been calculated due to peak overlap. The data will soon be available to the scientific community via the IBANDL website (<https://www-nds.iaea.org/exfor/ibandl.htm>).

References

- [1] V. Foteinou et al., Nucl. Instr. And Meth. In Phys. B 269, p. 2990 (2011)
- [2] P. Paul, K. P. Lieb, Nucl. Phys. 53, p. 465 (1964)
- [3] Chia-Shou Lin et al., Nucl. Phys. 275, p.93 (1977)
- [4] S.Harissopoulos et al., Eur. Phys. J. A – Hadrons Nuclei 9 , p. 479 (2000)
- [5] C. Kalfas, M. Axiotis, C. Tsabaris, Nucl. Instr. And Meth., A 830 , p. 265 (2016)
- [6] M. Mayer, AIP Conf. Proc. 475, p. 541 (1999)
- [7] V. Foteinou et al., Nucl. Instr. And Meth., B 396, p. 1 (2017)
- [8] A. Gurbich, Nucl. Instr. And Meth. In Phys. B, 371, p. 27 (2016)
- [9] M. Kokkoris et al., Nucl. Instr. And Meth. In Phys. B 254 , p. 10 (2007)